09

Capsule gas-filled target for a laser-plasma EUV source

© A.Ya. Lopatin,[1] A.N. Nachay,[1] A.A. Perekalov,[1] A.E. Pestov,[1] A.A. Soloviev,[2]
N.N. Tsybin,[1] N.I. Chkhalo,[1] D.S. Dmitriev,[1]

[1]Institute of Physics of Microstructures, Russian Academy of Sciences,
7607680 Nizhny Novgorod, Russia
[2]Institut prikladnoy fiziki RAN,
603950 Nizhny Novgorod, Russia
e-mail: lopatin@ipm.sci-nnov.ru

Received May 14, 2024
Revised May 14, 2024
Accepted May 14, 2024

A new design of a laser target — a container with a thin-film wall containing a gas under significant pressure is proposed. It is assumed (and this assumption will be tested experimentally), that, with a certain combination of design parameters, lines belonging to the gas enclosed in the target volume will prevail in the spectrum of extreme ultraviolet radiation of a laser-plasma source with such a target. The necessary experimental equipment has been developed and manufactured, including a set of identical targets with a $Mo/ZrSi_2$ membrane with a thickness of $0.19\,\mu$m. It has been experimentally demonstrated that the samples from the manufactured kit withstand a pressure of at least 1.5 atm.

Keywords: SXR and EUV radiation, thin films, laser plasma, gas target.

DOI: 10.61011/TP.2024.07.58815.170-24

Introduction

Submicron films are considered the best solid-state targets or many laser-plasma experiments. The study of laser generation opportunities at extreme ultraviolet (EUV) and tender X-ray (TX) wavelengths in plasma generated by laser pulse on a solid body surface used targets in the form of thin plasma-forming substance layers applied to thin polymer film to achieve more uniform distribution of concentration over the plasma channel cross section and to avoid refraction [1–4]. The experiments on hard X-ray plasma radiation generated at typical intensities of incident laser beam higher than $10^{14}\,W/cm^2$ use targets in the form of individual or stacked thin films [5,6] to achieve higher temperature of the radiating plasma and improve the performance of such sources.

For a long period of time, the Institute of Physics of Microstructures, Russian Academy of Sciences, (IPM RAS) has been developing a powerful technique for manufacturing thin-film EUV absorption filters — metallic films with typical thicknesses from 0.1 to $1\,\mu$m that are free-hanging or bonded to a support grid. The recent studies [7,8] reported that films were made from some materials (Be, C, Al, Si) in the form of laser targets of $0.1\,\mu$m in thickness and testing results were obtained for such targets on an EUV laser-plasma test bench; focused laser pulse intensity was about $10^{12}\,W/cm^2$ that was limited by the capabilities of available equipment. The main finding of the test is that thin films give lower yield of EUV radiation than one-piece targets from the same materials, but the difference is not too substantial (from 1.5 to 4 times depending on the target material and spectral interval).

Gas targets have even more extensive application in experiments on interaction between powerful laser radiation and substance. They are not only widely used in studies of EUV and TX laser-plasma sources, but are also employed for most implementations of high laser radiation harmonics [9–12] and also for experiments on laser-plasma acceleration of charged particles [13–16]. A gas jet flowing into vacuum from a nozzle equipped with a pulse valve is most often used as a gas target. Another design is a gas cell consisting of a small cavity that is filled with stationary gas flux and has a couple of small holes on two opposite ends (or with a hole on one of them if the laser beam is focused into the cell through a transparent window). Gas cells are preferred for high-order harmonic generation devices because they can provide much higher conversion efficiency than that achieved when using jet targets [12].

To study the laser-plasma bands of an EUV radiation source with a gas jet target, the Institute of Physics of Microstructures, Russian Academy of Sciences, is focused on the search for conditions ensuring maximum radiation yield in a reflection wavelength band of multilayer coating with a central wavelength of 13.5 nm or 11.2 nm. At these wavelengths, Mo/Si- or Mo/Be-based multilayer mirrors, respectively, are able to provide reflectances more than 70%, which is the basis for selection of one of them as an operating wavelength for projection nanolithography tools. It has been experimentally found that the maximum radiation intensity of the source in this spectral range may be achieved when using xenon as a plasma-forming gas. However, the spectral absorption peak of neutral xenon atoms in the EUV range also falls on a wavelength interval that is interesting for lithography. This factor, taking into

account very nonuniform distribution of gas concentration in the vicinity of the jet, may hinder reliable estimate of laser radiation conversion efficiency in EUV and be one of the reasons for nonconformity of xenon-target sources reported by various research teams [17–19].

A concept of a new type of gas target is proposed herein — a sealed gas-filled capsule a part of enclosure of which is made as a thin-film membrane that serves to input laser radiation and is destroyed by the arriving pulse. In this case, the EUV spectrum of the source shall contain multicharged ion lines both of the membrane material and of the gas downstream of the membrane. Moreover, it can be expected that a particular combination of membrane material and gas filling will result in considerable difference of the spectrum from simple overlap of two partial components because plasma ionization and heating are performed in a more sophisticated way. In particular, a contribution may be made by membrane substance ion recharging processes on gas atoms that were reliably observed in the experiments with plasma transit from a laser-irradiated solid-state target through a nearby gas jet [20].

In terms of practical application of capsule targets, we suppose that the options with petawatt laser systems may be the most promising for the experiments on higher harmonic generation and charged particle acceleration in the charge-separation field that accompanies the laser pulse. The use of capsule type targets as part of laser-plasma EUV radiation sources with low-cost high pulse repetition rate lasers is not cost-effective due to considerable efforts required for capsule manufacturing. On the other hand, as mentioned above, the effect of absorption of the EUV radiation from a jet-target source in the surrounding gas cloud on the performance of such source in the wavelength range of 11–13 nm is an important problem. For a capsule target, such absorption is minimized because gas leakage is avoided until the membrane is destroyed by the laser pulse and for the same reason gas concentration in the laser exposure area is characterized by a single particular value that shall simplify the interpretation of findings. Therefore the laser and test equipment available with the Institute of Physics of Microstructures, RAS, will be used to investigate the EUV radiation generation efficiency and spectral composition when the capsule target is exposed to nanosecond laser pulses. The obtained data will be useful for numerical simulation of the experimental findings. Prediction reliability of the brightness ans spectral properties of the EUV source with a new type of target based only on calculations without reference to experimental data seems to be questionable.

1. Fabrication of capsule type laser targets

Practical utilization of capsule targets in the EUV radiation generation experiment may be hindered by fast gas loss from the capsule volume due to the diffusion through thin film during long-term vacuum pumping. To overcome this hindrance, the capsule shall be filled with gas directly before utilization — in the vacuum chamber within a short period of time before the laser pulse. In such case, the capsule target design includes a sealed volume formed by a solid housing and a thin-wall membrane, and holes for supply of gas isolated from the gas pipeline by a shutoff valve. Considering the foregoing, it was decided to use a cylindrical small cross-section tube sealed on one end by the bonded thin-film membrane; the opening on the other end serves to fill the capsule with the operating gas. The gas-filled capsule will be sealed by rubber seals. The brass tube with OD 2 mm and ID 1.4 mm (wall thickness 0.3 mm) was divided into 12.5 mm lengths suitable for target handling during strength testing of a thin-film window and also in future experiments for investigation of spectra of such targets in the EUV band.

A 0.19 μm Mo/$ZrSi_2$ multilayer structure was proposed as a thin-film membrane for the input window. This structure was chosen because it has higher mechanical strength compared with multilayer free-hanging films made from materials with a lower atomic number that are the best for spectral examination. In this case, it was important to demonstrate that the capsule can be pressurized to a pressure much higher than the atmosphetic pressure. The membrane was made using a wide-aperture thin-film EUV filter fabrication technique utilized by IPM RAS [21] that includes magnetron sputtering stages for application of a film (future thin-film membrane) and a sacrificial layer to a polished Si substrate (surface roughness about 0.3 nm), removal of the sacrificial layer during liquid etching with separation of the film from the substrate and film catching from the liquid surface onto a supporting frame.

To perform the studies, preferably use simultaneous charging of a set of targets into the vacuum chamber, this will help conduct a measurement series (examine the dependence of the EUV radiation properties of the capsule targets on various parameters — laser pulse energy, gas pressure in the capsule) without opening the capsule to atmosphere in order to replace the capsule target. A set of targets (about 60 pieces) was made by a group method. Pieces of tubes were placed vertically into a templet consisting of a set of densely spaced holes in a plate — each work piece of the future target (a tube of 12.5 mm in length) was inserted in the appropriate hole, tube ends protruded above the plate to an equal distance. A thin epoxy adhesive layer was applied to the tube ends, then this assembly was placed on a bench that provided smooth movement with respect to a fixed film membrane workpiece and engaged with the latter such that the membrane turned to be tightly bonded to the tube ends. After epoxy adhesive curing, the thin film was destroyed in spaces between the tubes and the assembly was separated into individual finished targets. Figure 1 shows the photographs of the set of capsule targets before the membrane adhesion and before and after the film failure in the spaces between individual tubes.

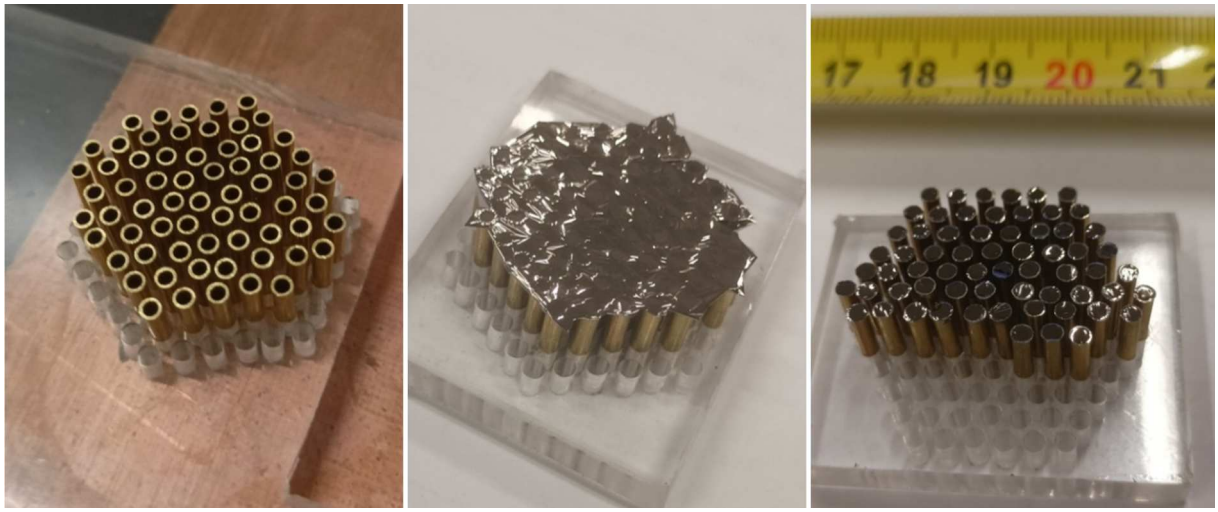

Figure 1. Photos of capsule target fabrication stages.

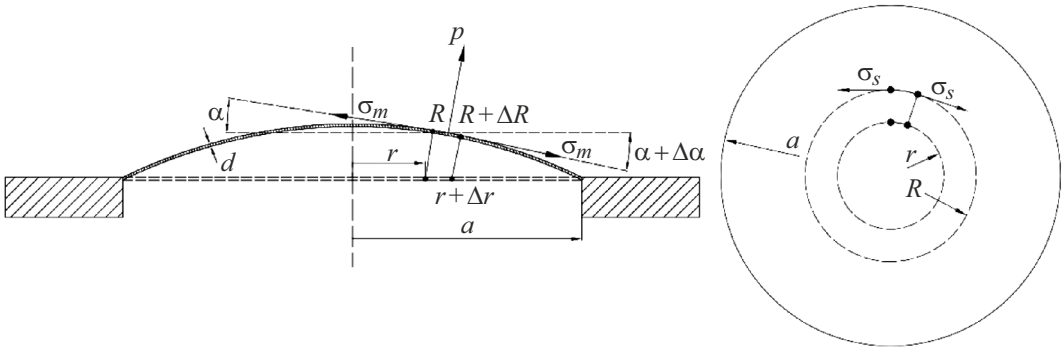

Figure 2. Forces applied to the stretched membrane; left — in radial cross section, right — in azimuthal direction. a, r, R are counted from the tube center line, a is the tube radius.

2. Strength properties of the capsule target membranes

To solve the problem of elastic deformation of a thin-film membrane under the applied differential pressure, we used a model where the external pressure applied to the surface is balanced exclusively by tension of the material in the film plane. The contribution of stresses associated with shear and bending deformations that are usually significant for thicker plates may be neglected. Use indices m and s or deformations ε and stresses σ of a rounds membrane loaded by the external pressure p, respectively, in radial and azimuthal directions. Some introduced symbols are shown in Figure 2.

Generalized Hooke's law may be written as the following pair of relations:

$$\varepsilon_m = \frac{1}{E} \cdot [\sigma_m - \nu \cdot (\sigma_s + \sigma_z)],$$

$$\sigma_s = \frac{1}{E} \cdot [\sigma_s - \nu \cdot (\sigma_m + \sigma_z)],$$

where E is Young's modulus, ν is Poison's ratio, σ_z is the stress component normal to the specimen. Since the problem has no external forces applied for membrane compression or tension in thickness, σ_z may be assumed as equal to zero (a so-called plane stress state was implemented). Considering this, an expression for σ_m may be derived easily:

$$\sigma_m = \frac{E}{1-\nu^2} \cdot [\varepsilon_m + \nu \cdot \varepsilon_s].$$

The same expression is used to define the azimuthal stress component σ_s. The following symbols will be used for membrane deflection analysis: r is the radius in the polar coordinate system of a point on the unstressed (initial) membrane, R is the radius to which this point goes after membrane loading by external pressure, α is the inclination angle between the radial tangent line to the deflected membrane and initial plane, d is the film thickness. Two balance conditions of a differentially small membrane element — with respect to normal displacement and with respect to radial displacement — may be written as follows:

$$\sigma_m \cdot d \cdot \alpha' = p \cdot (1 + \varepsilon_m),$$

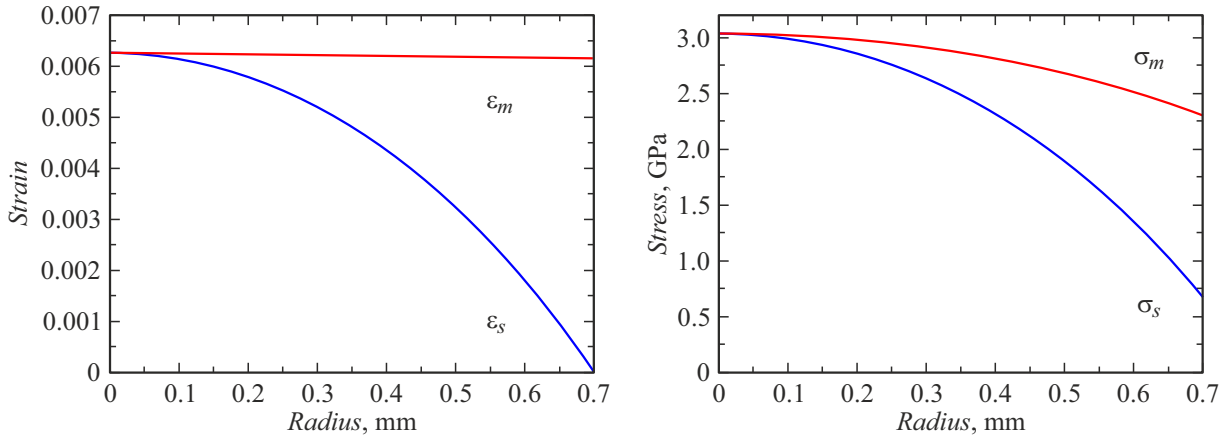

Figure 3. Dependences of elongation and stress components on radius obtained within the used model for the following values: $d = 0.19\,\mu$m, $E = 340$ GPa, $\nu = 0.3$, $P = 150$ kPa.

$$(\sigma_m \cdot R)' = \sigma_s \cdot (1 + \varepsilon_m).$$

The prime mark here denotes a derivative with respect to radius. The first of the relations expresses the external pressure compensation due to the occurrence of a normal projection of radial bend tension of the element of interest. The second relation — is the internal stress compensation condition in the film that ensures radial stability of the element. Finally, another two equations written below determine local radial and azimuthal elongations:

$$R' = (1 + \varepsilon_m) \cdot \cos(\alpha),$$

$$\varepsilon_s = \frac{R}{r} - 1.$$

The obtained relations are limited to a system of three differential equations that is quite simple for numerical solution:

$$\varepsilon_s' = \frac{1}{r} \cdot [(1 + \varepsilon_m) \cdot \cos(\alpha) - \varepsilon_s - 1],$$

$$\alpha' = \frac{p \cdot (1 - \nu^2)}{E \cdot d} \cdot \frac{1 + \varepsilon_m}{\varepsilon_m + \nu \cdot \varepsilon_s},$$

$$(\varepsilon_m + \nu \cdot \varepsilon_s)' = \frac{1}{r} \cdot \frac{1 + \nu_m}{1 + \varepsilon_s}$$

$$\times [\varepsilon_s \cdot (1 - \nu \cdot \cos(\alpha)) + \varepsilon_m \cdot (\nu - \cos(\alpha))].$$

One of the boundary conditions for this system ($\varepsilon_s = 0$) is defined on the outer contour of the membrane, and $\varepsilon_s = \varepsilon_m$ shall be satisfied on the zero radius. The simplest way to find the solution — is to select such elongations in the center of the membrane that will provide ε_s equal to zero on the outer contour at the set external parameters (pressure, dimensions of the specimen and elastic moduli of the material).

Figure 3 shows the examples of solution — curves of the radial dependences of deformation and stress components in a round membrane. Stress within the model turns to be maximum in the center. According to [22], this conclusion is also supported by membrane stress counting in COMSOL software. However, note that a higher stress than in the center may occur on the narrow ring on the attachment outline in case of a sharp edge (i.e. if the attachment outline has a form of right angle without any vertex rounding).

Deflection of thin films under external pressure is often described using an approximate approach based on the assumptions concerning a strictly spherical shape of the deflected membrane and stress constancy throughout the deflection surface. Within this approach, analytical expressions correlating the deflection, elongation and mechanical stress with external pressure may be derived. The experimentally recorded dependence of deflection on pressure may be used to estimate the biaxial modulus of elasticity Y defined as $Y = E/(1 - \nu)$. Y has been found and strength properties of those thin-film membranes that are most widely used as EUV filters have been investigated by us earlier [23–25]. In particular, Mo/$ZrSi_2$ multilayer film with the same material thicknesses (2.5 nm in molybdenum layers and 1.5 nm in zirconium silicide layers) as those of the film used herein for fabrication of the capsule target specimens was also examined. Biaxial modulus of elasticity of such multilayer structure was estimated as 340 GPa, whereas the ultimate strength was estimated as 0.8–1.3 GPa.

Using the equations given in [23], the correlation between the pressure applied to the film p and mechanical stress σ occurring in the material may be written as:

$$p = \frac{4 \cdot d}{a} \cdot \sqrt{\frac{2 \cdot \sigma^3}{Y}},$$

where a a is the film radius, d is the film thickness. We estimate the value of σ at which film failure is possible as Y/200 — such relation of the ultimate strength to the elastic modulus is typical for metals. Then, for the membrane thickness $d = 0.19\,\mu$m and radius $a = 0.7$ mm, we get the maximum pressure limit that can be withstood by the specimen equal to $1.6 \cdot 10^5$ Pa.

Figure 4. Photographs of the test bench (left) and film specimen testing (right).

To test the capsule target film window at a differential pressure higher than 1 atm, a test bench was fabricated (Figure 4, left) and connected to a 6 atm compressed air line. The test bench consisted of a buffer tank, shutoff valve for smooth air supply and release, flange for attachment of the test specimen (vacuum sealing was ensured on the external surface of the cylinder using a rubber O-ring) and an indicating pressure gauge with the measurement range of 1.5 atm. Three specimens were tested and all them withstood the differential pressure of 1.5 atm without failure. Photograph of a specimen attached to the test bench flange during the measurements in shown in Figure 4, right.

Thus, the theoretical prediction concerning the capability of the $0.19\,\mu$m Mo/$ZrSi_2$ multilayer membrane to withstand a differential pressure of at least 1.5 atm at the membrane diameter of 1.4 mm is verified experimentally.

3. Test bench for examination of emission properties of capsule targets

To study emission spectra of the capsule targets with laser excitation compared with those of the gas jet flowing into the vacuum volume, an experiment is to be performed using the setup as shown in Figure 5. In the first case, a capsule target is placed in the laser radiation focusing area (targets from the set are fed successively), in the second case, the laser pulse is focused on a gas jet flowing into vacuum. Nd:YAG laser with a pulse energy of 0.8 J and a pulse width of 5 ns is expected to be used for the experiment, the lens will then achieve the intensities in the focus up to $3 \cdot 10^{12}$ W/cm^2 with a typical focusing spot size of $70\,\mu$m. Simplified representation of the interaction between the laser pulse and capsule target is as follows: leading edge of the arriving pulse destroys the thin-film membrane, and the main part of the pulse interacts with the working gas — multiple ionization of atoms takes place and is followed by the radiative recombination and photon emission in the EUV wavelength band.

The EUV radiation flux is recorded using a mirror spectrometer [26] with replaceable mirrors covering the wavelength range of 6–30 nm. Spectral resolution of the instrument within the spectral range is 0.1–0.9 nm (depending on the spectral bandpass of the multilayer X-ray mirror). The instrument is equipped with a EUV detector (FDUK-100UV silicon photodiode) calibrated on BESSY II synchrotron. TX and EUV bandwidth spectral sensitivity of the detector is described in [27].

Wavelength scanning is performed by rotating the multilayer monochromator mirror at a an angle φ with simultaneous detector rotation at an angle 2φ from the initial position corresponding to the source, mirror and detector position in line. In this case, the angle of incidence on the multilayer mirror will be equal to the angle of reflection towards the detector. The detector records a signal at a wavelength for which Wulff–Bragg's condition is satisfied:

$$2d \cdot \sin\varphi = \lambda,$$

Where d is the multilayer mirror period, φ is the angle of radiation incidence, λ is the wavelength.

To perform the experiment as described above, the capsules shall be preferably filled with the working gas immediately before use. Otherwise, it is difficult to control pressure in the capsule target that can decrease significantly during the vacuum pumping period due to gas diffusion through the thin-film membrane. A specialized bench has been developed to avoid this problem. The bench provides charging of quite many capsules within one vacuum pumping cycle, successive supply of targets into the laser focusing area, filling each capsule with gas after placement in the focus area — with a short time interval before the laser pulse. The test bench drawing is shown in Figure 6.

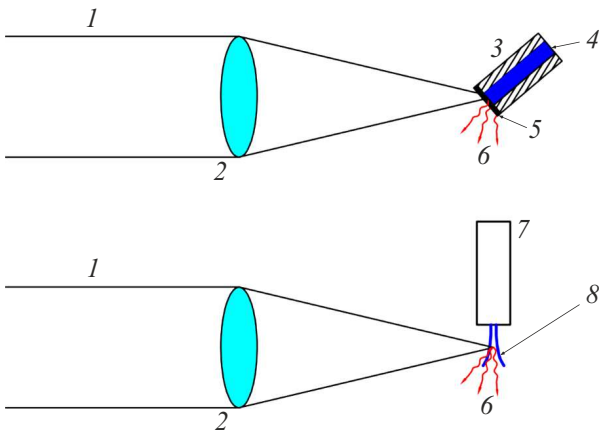

Figure 5. Experimental setup for examination of the EUV radiation generation at laser excitation of the capsule target (upper) and gas jet (lower). *1* — laser beam, *2* — lens, *3* — capsule target, *4* — gas supply, *5* — thin film, *6* — X-ray radiation, *7* — gas nozzle, *8* — gas jet.

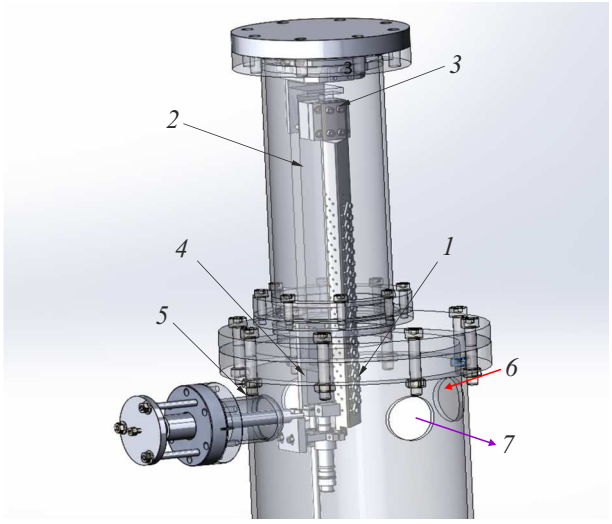

Figure 6. 3*D* visualization of the test bench for the investigation of EUV radiation of capsule targets. *1* — capsule target placed in the laser focusing area, *2* — bar with a set of capsules attached to it, *3* —vertical movement drive for the bar with targets, *4* — gas valve, *5* — actuating valve rod, *6* — laser pulse inlet, *7* — EUV pulse outlet from the target to the mirror spectrometer.

Eighteen capsule targets are installed on the bar — V-shaped bar with its one side attached to a linear motor-driven translator. The number of targets is limited by the chamber height and translator travel. Through holes are drilled through two other sides of the bar. Capsule targets are attached on one side in the retainer plate holes and sealed on the external surface of the cylinder using a rubber seal. The gas valve is secured on the actuating rod designed to press tightly the valve outlet with a rubber seal to the highly polished side of the bar with the open hole ends on it. The gas line is equipped with a piezoresistive sensor designed for continuous pressure control in the capsule (the sensor is not shut off from the capsule volume when the gas filling process is completed). The target is filled with gas as follows. The capsule is moved into the laser focusing area by the motor-driven linear translator. The gas valve is brought to the bar with capsule targets by the actuating rod and pressed to it to ensure tight connection. The valve is opened and a metered flow of gas is fed into the capsule with pressure control. When the required pressure has been achieved, the gas valve is closed and then the capsule target is used, i.e. exposed to the laser pulse. Then the process is repeated until all installed targets are depleted

Due to simultaneous charging of many capsules and prompt gas pressure control, the designed bench will reduce significantly the recording time of EUV radiation spectra from the plasma source with a new type of targets. For comparison with the radiation spectra of the laser targets with gas jets flowing into vacuum, the bench involves replacement of the capsule feeder with a pulsed gas nozzle fixed near the laser focusing area.

Conclusion

The study proposes a new type of laser targets — gas-filled capsule-type targets with a thin-film membrane destroyed by the laser pulse. Design in the form of thick-wall tubes ($Ø_{outer} = 2\,mm$, $Ø_{inner} = 1.4\,mm$) with a $0.19\,\mu m$ Mo/$ZrSi_2$ multilayer film membrane bonded to one of the ends. The opposite end of the tube remains open to fill the capsule with gas inside the vacuum volume immediately before use. Capability of the membrane to withstand a differential pressure higher than 1.5 atm has been predicted theoretically. This prediction has been verified experimentally. Installation of the experimental bench of the EUV source with capsule targets is currently performed, the vacuum chamber has been made, exciting laser and gas supply system has been installed. Tightness test of the chamber has been completed, the mirror spectrometer has been mounted. In the nearest future, the system for feeding targets into the laser interaction area is to be installed and the irradiative properties are to be studied. Inert gas (Ar, Kr, Xe) radiation spectra will be studied in the wavelength range of $6-30\,nm$ depending on the gas pressure in the capsule compared with the radiation spectra of the targets in the form of a gas jet flowing from a nozzle.

Finally, it should be noted that the developed targets are also suitable for those applications where the gas emission lines are excited by and electron beam, rather than by laser exposure. The beam intensity may not be very high — not to destroy the film window. The advantages of metallic films over polymer films in such applications are obvious — they do not accumulate charge, are not depolymerized by the flowing electron beam and remove absorbed heat adequately. He II ($\lambda = 30.4\,nm$) radiation source may be used as a specific example of such application. Sources at this wavelength are used for photoelectron spectroscopy and are usually helium glow discharge instruments [28] that have no high brightness. We believe that an interesting alternative includes a source where helium filled in the capsule at high pressure is ionized by the electron beam input through the thin-film window, and radiation via the 30.4 nm line is also output through a thin-film Al window that has a transmission of about 50% at this wavelength at a thickness of $0.1\,\mu m$.

Funding

The study was supported financially by the Ministry of Science and Higher Education of the Russian Federation (agreement № 075-15-2021-1361).

Conflict of interest

The authors declare that they have no conflict of interest.

References

[1] M.D. Rosen, P.L. Hagelstein, D.L. Matthews, E.M. Campbell, A.U. Hazi, B.L. Whitten, B. MacGowan, R.E. Turner, R.W. Lee, G. Charatis, G.E. Busch, C.L. Shepard, P.D. Rockett. Phys. Rev. Lett., **54** (2), 106 (1985). DOI: 10.1103/PhysRevLett.54.106

[2] S. Maxon, P. Hagelstein, J. Scofield, Y. Lee. J. Appl. Phys., **59** (1), 293 (1986). DOI: 10.1063/1.336834

[3] T.N. Lee, E.A. McLean, R.C. Elton. Phys. Rev. Lett., **59** (11), 1185 (1987). DOI: 10.1103/PhysRevLett.59.1185

[4] M. Nishikino, Yo. Ochi, N. Hasegawa, T. Kawachi, H. Yamatani, T. Ohba, T. Kaihori, K. Nagashima. Rev. Sci. Instrum., **80** (11), 116102 (2009). DOI: 10.1063/1.3262634

[5] D. Babonneau, M. Primout, F. Girard, J.-P. Jadaud, M. Naudy, B. Villette, S. Depierreux, C. Blancard, G. Faussurier, K.B. Fournier, L. Suter, R. Kauffman, S. Glenzer, M.C. Miller, J. Grün, J. Davis. Phys. Plasmas, **15** (9), 092702 (2008). DOI: 10.1063/1.2973480

[6] Sh.-Yo. Tu, G.-Yu. Hu, W.-Yo. Miao, B. Zhao, J. Zheng, Yo.-T. Yuan, X.-Yu Zhan, L.-F. Hou, Sh.-E. Jiang, Yo.-K. Ding. Phys. Plasmas, **21** (4), 043107 (2014). DOI: 10.1063/1.4871730

[7] S.A. Garakhin, A.Ya. Lopatin, A.N. Nechay, A.A. Perekalov, A.E. Pestov, N.N. Salashchenko, N.N. Tsybin, N.I. Chkhalo. Tech. Phys., **67** (8), 1015 (2022) DOI: 10.21883/TP.2022.08.54565.75-22

[8] A.Ya. Lopatin, V.I. Luchin, A.N. Nachay, A.A. Perekalov, A.E. Pestov, N.N. Salashchenko, A.A. Soloviev, N.N. Tsybin, N.I. Chkhalo. Tech. Phys., **68** (7), 829 (2023). DOI: 10.61011/TP.2023.07.56623.97-23

[9] A. L'Huillier, P. Balcou. Phys. Rev. Lett., **70** (6), 774 (1993). DOI: 10.1103/PhysRevLett.70.774

[10] C.-G. Wahlström, J. Larsson, A. Persson, T. Starczewski, S. Svanberg, P. Saliéres, Ph. Balcou, A. L'Huillier. Phys. Rev. A, **48** (6), 4709 (1993). DOI: 10.1103/PhysRevA.48.4709

[11] J. Zhou, J. Peatross, M.M. Murnane, H.C. Kapteyn, I.P. Christov. Phys. Rev. Lett., **76** (5), 752 (1996). DOI: 10.1103/PhysRevLett.76.752

[12] J.-P. Brichta, M.C.H. Wong, J.B. Bertrand, H.-C. Bandulet, D.M. Rayner, V.R. Bhardwaj. Phys. Rev. A, **79** (3), 033404 (1993). DOI: 10.1103/PhysRevA.79.033404

[13] D. Guénot, D. Gustas, A. Vernier, B. Beaurepaire, F. Böhle, M. Bocoum, M. Lozano, A. Jullien, R. Lopez-Martens, A. Lifschitz, J. Faure. Nature Photon., **11** (5), 293 (2017). DOI: 10.1038/nphoton.2017.46

[14] A. Pak, K.A. Marsh, S.F. Martins, W. Lu, W.B. Mori, C. Joshi. Phys. Rev. Lett., **104** (2), 025003 (2010). DOI: 10.1103/PhysRevLett.104.025003

[15] N. Delbos, C. Werle, I. Dornmair, T. Eichner, L. Hübner, S. Jalas, S.W. Jolly, M. Kirchen, V. Leroux, P. Messner, M. Schnepp, M. Trunk, P.A. Walker, P. Winkler, A.R. Maier. Nucl. Instrum. Methods Phys. Res. A, **909**, 318 (2018). DOI: 10.1016/j.nima.2018.01.082

[16] H.-E. Tsai, K.K. Swanson, S.K. Barber, R. Lehe, H.-Sh. Mao, D.E. Mittelberger, S. Steinke, K. Nakamura, J. van Tilborg, C. Schroeder, E. Esarey, C.G.R. Geddes, W. Leemans. Phys. Plasmas, **25** (4), 043107 (2018). DOI: 10.1063/1.5023694

[17] H. Komori, Y. Ueno, H. Hoshino, T. Ariga, G. Soumagne, A. Endo, H. Mizoguchi. Appl. Phys. B., **83** (2), 213 (2006). DOI: 10.1007/s00340-006-2172-7

[18] V.P. Belik, S.G. Kalmykov, A.M. Mozharov, M.V. Petrenko, M.E. Sasin. Tech. Phys. Lett., **43** (12), 1001 (2017). DOI: 10.1134/S1063785017110177

[19] A.N. Nechay, A.A. Perekalov, N.N. Salashchenko, N.I. Chkhalo. Opt. i spektr., **129** (3), 266 (2021). (in Russian) DOI: 10.21883/OS.2021.03.50652.282-20

[20] I.L. Beigman, E.A. Vishnyakov, M.S. Luginin, E.N. Ragozin, I.Yu. Tolstikhina. Quantum Electron., **40** (6), 545 (2010). DOI: 10.1070/QE2010v040n06ABEH014313

[21] B.A. Volodin, S.A. Gusev, M.N. Drozdov, S.Yu. Zuev, E.B. Klyuenkov, A.Ya. Lopatin, V.I. Luchin, A.E. Pestov, N.N. Salashchenko, N.N. Tsybin, N.I. Chkhalo. Bull. Russ. Acad. Sci. Phys., **74** (3), 46 (2010). DOI: 10.3103/S1062873810010120

[22] J.D. Baek, Y.J. Yoon, W. Lee, P.-Ch. Su. Energy Environ. Sci., **8** (11), 3374 (2015). DOI: 10.1039/C5EE02328A

[23] N.I. Chkhalo, E.B. Kluenkov, A.Ya. Lopatin, V.I. Luchin, N.N. Salashchenko, L.A. Sjmaenok, N.N. Tsybin. Thin Solid Films, **631**, 93 (2017). DOI: 10.1016/j.tsf.2017.04.015

[24] N.I. Chkhalo, S.V. Kuzin, A.Ya. Lopatin, V.I. Luchin, N.N. Salashchenko, S.Yu. Zuev, N.N. Tsybin. Thin Solid Films, **653**, 359 (2018). DOI: 10.1016/j.tsf.2018.03.051

[25] S.Yu Zuev, E.B¿ Klyuenkov, A.Ya. Lopatin, V.I. Luchin, D.G. Pariev, R.S. Pleshkov, V.N. Polkovnikov, N.N. Salashchenko, M.V. Svechnikov, N.N. Tsybin, N.I. Chkhalo. Kharakterizatsiya absorbtsionnykh filtrov EUF izlucheniaya na osnove plenok berilliya submikronnoy tolshchiny. (Tr. XXII simp. „Nanofizika i nanoelektronika“ t. 1, s. 438 (2018) (in Russian)

[26] A.V. Vodop'yanov, S.A. Garakhin, I.G. Zabrodin, S.Yu. Zuev, A.Ya. Lopatin, A.N. Nechay, A.E. Pestov, A.A. Perekalov, R.S. Pleshkov, V.N. Polkovnikov, N.N. Salashchenko, R.M. Smertin, B.A. Ulasevich, N.I. Chkhalo. Quantum Electron., **51** (8), 700 (2021). DOI: 10.1070/QEL17598

[27] P.N. Aruev, M.M. Barysheva, B.Ya. Ber, N.V. Zabrodskaya, V.V. Zabrodskii, A.Ya. Lopatin, A.E. Pestov, M.V. Petrenko, V.N. Polkovnikov, N.N. Salashchenko, V.L. Sukhanov, N.I. Chkhalo. Quantum Electron., **42** (10), 943 (2012). DOI: 10.1070/QE2012v042n10ABEH014901

[28] L.L. Coatsworth, G.M. Bancroft, D.K. Creber, R.J.D. Lazier, P.W.M. Jacobs. J. Electron Spectros. Relat. Phenomena, **13** (3), 395 (1978). DOI: 10.1016/0368-2048(78)85043-9

Translated by E.Ilinskaya